Harmful Algae 78 (2018) 75–85

Contents lists available at ScienceDirect

Harmful Algae

journal homepage: www.elsevier.com/locate/hal

Sympatric occurrence of two *Azadinium poporum* ribotypes in the Eastern Mediterranean Sea

Zhaohe Luo[a], Bernd Krock[b], Antonia Giannakourou[c], Amalia Venetsanopoulou[c], Kalliopi Pagou[c], Urban Tillmann[b,*], Haifeng Gu[a,*]

[a] Third Institute of Oceanography, State Oceanic Administration, Xiamen 361005, China
[b] Alfred Wegener Institute for Polar and Marine Research, Am Handelshafen 12, D-27570 Bremerhaven, Germany
[c] Hellenic Center for Marine Research, Institute of Oceanography, Attica 19013, Greece

ARTICLE INFO

Keywords:
Azadinium
Azaspiracid
AZA-2
AZA-40
Biogeography
Greece
Growth

ABSTRACT

The marine dinoflagellate *Azadinium poporum* produce azaspiracids (AZA) and has been recorded widely in the world. However, information on its biogeography is still limited, especially in view of the fact that *A. poporum* comprises several genetically differentiated groups. A total of 18 strains of *A. poporum* were obtained from the Eastern Mediterranean area by incubating surface sediment collected from Ionian Sea of Greece. The morphology of these strains was examined with light microscopy and scanning electron microscopy. Small subunit ribosomal DNA (SSU rDNA), large subunit ribosomal DNA (LSU rDNA) and internal transcribed spacer (ITS) sequences were obtained from all cultured strains. Molecular phylogeny based on concatenated SSU, LSU and ITS sequences confirmed three ribotypes within *A. poporum* and revealed two subclades within ribotypes A and C. Greek strains of *A. poporum* ribotype A were nested within ribotype A2 together with strains from Western Mediterranean Sea and French Atlantic, and Greek strains of *A. poporum* ribotype C were nested within ribotype C2 together with a strain from the Gulf of Mexico. Growth experiments on four selected strains revealed that ribotypes A and C from Greece differed in their growth at higher temperatures, indicating that they are physiologically differentiated. Azaspiracid profiles were analyzed for 15 cultured *A. poporum* strains using LC–MS/MS and demonstrate that the *A. poporum* ribotype A from Greece produce low level or no AZA and *A. poporum* ribotype C from Greece produces predominantly AZA-40 (9.6–30.2 fg cell^{-1}) followed by AZA-2 (2.1–2.6 fg cell^{-1}). The first record of AZA-40 producing *A. poporum* from the Mediterranean suggests that this species is a potential source for azaspiracid contaminations in shellfish from the Eastern Mediterranean Sea.

1. Introduction

The planktonic dinophyte *Azadinium spinosum* Elbrächter & Tillmann is the type species of the genus *Azadinium* Elbrächter & Tillmann, which for most species is characterized by a plate pattern of Po, cp, X, 4′, 3a, 6″, 6C, 5S, 6‴, 2⁗ (Tillmann et al., 2009). Slightly varying epithecal plate pattern were found in two other species, i.e. in *Azadinium dalianense* Z.Luo, H.Gu & Tillmann possessing three apical and two anterior intercalary plates (3′, 2a) (Luo et al., 2013) and in *Azadinium zhuanum* Z.Luo, H.Gu & Tillmann possessing four apical and two anterior intercalary plates (4′, 2a) (Luo et al., 2017a). In the molecular phylogeny however, *Azadinium* is monophyletic, forming the family Amphidomataceae together with the genus *Amphidoma* Stein (Tillmann et al., 2012; Luo et al., 2017a).

The toxigenic species *Azadinium poporum* has been recorded more widely than any other *Azadinium* species but still its presence in many areas has not been examined yet. It was originally described from the North Sea (North Atlantic) off Denmark (Tillmann et al., 2011) and now is known to comprise three genetically different but morphologically indistinguishable ribotypes (Gu et al., 2013). Strains from Denmark, French Atlantic, French Mediterranean, Chile, Pacific USA and New Zealand have been classified within ribotype A (Kim et al., 2017; Luo et al., 2017a; Tillmann et al., 2017b), whereas strains from Asian Pacific, Argentina, Gulf of Mexico were classified within ribotypes C (Tillmann et al., 2016; Luo et al., 2017a). Ribotype B was only reported in Chinese waters (Gu et al., 2013). Sympatric occurrence of two ribotypes of *A. poporum* was only reported in Chinese waters (ribotypes B and C, Gu et al., 2013). The presence of different ribotypes in the same area, however, might get unnoticed for other locations when only a limited number of strains are available.

* Corresponding authors.
E-mail addresses: urban.tillmann@awi.de (U. Tillmann), guhaifeng@tio.org.cn (H. Gu).

https://doi.org/10.1016/j.hal.2018.08.003
Received 27 April 2018; Received in revised form 2 August 2018; Accepted 3 August 2018

Compared to other *Azadinium* species, many more strains of *A. poporum* have been sequenced, but with new sequences from other localities additional ribotypes might be revealed. Some *A. poporum* strains of the same ribotype were found to share nearly identical LSU and ITS sequences although they originated from distant locations. For instance, *A. poporum* from New Zealand shared identical LSU sequences with those from Denmark (Smith et al., 2016). On the other hand, strains collected from close-by localities such as the French Atlantic and Danish Atlantic coasts may show some level of genetic differentiation even within the same ribotype (ribotype A) (Luo et al., 2017a). Whether further subdivisions of the ribotypes are justified remains to be determined.

Motile cells of *A. poporum* are relatively small ranging from 10 to 20 µm in cell length. Such small cells are easily overlooked in routine monitoring. To study the biogeography of *Azadinium*, molecular detection is promising, but specific probes have been designed for only a few species yet (Toebe et al., 2013) and they are only occasionally used (Smith et al., 2016; Kim et al., 2017). To evaluate the species specificity of previous molecular probes, it is essential to reveal genetic differentiation among strains from different area.

The first *Azadinium* species shown to produce azaspiracids (AZA) was *Azadinium spinosum* (Tillmann et al., 2009), and in Ireland this is the species responsible for cases of human intoxication via mussel consumption. Later, two other *Azadinium* species (*A. poporum* and *A. dexteroporum*) and one *Amphidoma* species (*Amphidoma languida*) were found to produce AZA, too (Krock et al., 2012; Gu et al., 2013; Rossi et al., 2017; Tillmann et al., 2017a). Initially, *Azadinium poporum* was described as a non-toxigenic species (Tillmann et al., 2011), but later it turned out that the type strain in fact produces a novel AZA (Krock et al., 2012), and that new strains of *A. poporum* from China produce diverse AZA, e.g. AZA-2, AZA-11, AZA-36, AZA-40 and AZA-41 (Krock et al., 2014). For *A. poporum* strains outside China, the AZA profiles are relatively uniform. AZA-37 is the only AZA reported yet in European Atlantic strains (Krock et al., 2012), whereas only AZA-2 (and low levels of AZA-2 phosphate) were detected in strains from Gulf of Mexico, Corsica of France and Argentina (Luo et al., 2016; Tillmann et al., 2016; Luo et al., 2017a). Likewise, only AZA-11 (and two phosphorylated AZA) were detected in Chilean strains (Tillmann et al., 2017b), and AZA-59 was the sole AZA detected in strains from Washington State, USA (Kim et al., 2017).

In the Mediterranean Sea, only two *Azadinium* species have been recorded. One strain of *Azadinium dexteroporum* has been described from the Gulf of Naples (Percopo et al., 2013), and was shown to produce seven (six of which were new to science) different AZA (Rossi et al., 2017). One strain of *A. poporum* was recovered in Corsica which is able to produce AZA-2 (Luo et al., 2017a), and an unidentified *Azadinium* species was encountered in water samples collected in Fangar Bay (Catalan coast, NW Mediterranean) (Busch et al., 2016), suggesting that higher diversity and wider distribution of *Azadinium* can be expected in the Mediterranean Sea. In addition, AZA-2 was detected in mussels collected in the Adriatic Sea in 2012 and 2013 (Bacchiocchi et al., 2015), but the responsible species has not been identified yet.

In ongoing attempts to complement *Azadinium* diversity and biogeography, 18 strains of *A. poporum* from the Ionian Sea of Greece were established. Cultured strains were examined for their morphology, and were analyzed for the presence of AZA. In addition, small subunit ribosomal DNA (SSU rDNA), partial large subunit ribosomal DNA (LSU rDNA) and internal transcribed spacer (ITS) sequences were determined for the cultured strains and molecular phylogeny was inferred using concatenated SSU, ITS and LSU rDNA sequences.

2. Material and methods

2.1. Sample collection and treatment

Sediment samples were collected from the Gulf of Amvrakikos (station 21) and Igoumenitsa (station 24) in 2014 using a grab (Table 1, Fig. S1). The Amvrakikos Gulf is a large (405 km^2), semi-enclosed embayment, located in Western Greece. It is connected to the open Ionian Sea through a narrow, elongated channel, the Preveza Straits, which is approximately 6 km long, 0.8 to 2.5 km wide and 20 m deep (Naeher et al., 2012). The mean depth of the gulf is 26 m, while the maximum depth of 63 m has been recorded in its eastern part (Kehayias and Aposporis, 2014). The Ionian Sea is an elongated bay of the Mediterranean Sea, south of the Adriatic Sea.

Station 21 is in its southern part of Amvrakikos gulf, near to Amfilochia town, and station 24 is located in the Igoumenitsa gulf (Epirus, Northern Greece), a sheltered enclosed mass of water in the Ionian Sea, with a shoreline of approximately 1.4 km in length (Beza et al., 2014). In the easternmost part of Igoumenitsa gulf is located the port of Igoumenitsa, one of the largest passenger ports in the Eastern Mediterranean Sea basin, which handles around one million passengers per year for international destinations.

The top 2 cm were sliced off and stored in the dark at 4 °C until further treatment. Approximately 5 g of wet sediment was mixed with 20 mL of 0.22 µm filtered seawater and stirred vigorously to dislodge detrital particles. The settled material was subsequently sieved through 120 µm and 10 µm filters. The 10–120 µm fractions were rinsed with f/2-Si medium (Guillard and Ryther, 1962) and transferred into a 96-well culture plate. The culture plate was incubated at 20 °C, 90 µmol quanta m^{-2} s^{-1} under a 12:12 h light: dark cycle (hereafter called "standard culture conditions"). Cells of *Azadinium* are characterized by swimming at low speed, interrupted by short, high-speed 'jumps' in various directions (Tillmann et al., 2009). Cells exhibiting such a characteristic swimming behavior were isolated with a micropipette under an inverted microscope Leica DMi1 (Leica, Wetzlar, Germany) and established in clonal cultures under standard culture conditions.

2.2. Light microscopy (LM)

Live cells were examined and photographed using a Zeiss Axio Imager microscope (Carl Zeiss, Göttingen, Germany) equipped with a Zeiss Axiocam HRc digital camera. Cell size of thirty cells was measured using Axiovision (4.8.2 version) software at ×1000 magnification. To observe the shape and location of the nucleus, cells were stained with 1:100 000 SYBR Green (Sigma Aldrich, St. Louis, USA) for 1 min, and photographed using the Zeiss fluorescence microscope with a Zeiss-38 filter set (excitation BP 470/40, beam splitter FT 495, emission BP 525/50).

Table 1
Azadinium poporum strains examined in the present study, including the ribotype, collection locality, coordinates, collection date and water depth.

Species	Strains	Ribotypes	Latitude (N)	Longitude (E)	Location	Collection date	Station	Depth (m)
A. poporum	TIO420-425	A	38°55'18.12"	21°05'42.36"	Amvrakikos/Ionian Sea	2014.09.27	21	42.5
A.poporum	TIO433-438	A	38°55'18.12"	21°05'42.36"	Amvrakikos/Ionian Sea	2014.09.27	21	42.5
A.poporum	TIO431, 432	A	39°30'13.68"	20°15'01.08"	Igoumenitsa/Ionian Sea	2014.09.28	24	22.9
A.poporum	TIO427-429	C	39°30'13.68"	20°15'01.08"	Igoumenitsa/Ionian Sea	2014.09.28	24	22.9
A. poporum	TIO452	C	39°30'13.68"	20°15'01.08"	Igoumenitsa/Ionian Sea	2014.09.28	24	22.9

2.3. Scanning electron microscopy (SEM)

Mid-exponential batch cultures were concentrated by a Universal 320 R centrifuge (Hettich-Zentrifugen, Tuttlingen, Germany) at 850 *g* for 10 min at room temperature. The cell pellet was treated as described by Tillmann et al. (2009) to strip off the outer cell membrane. Cells were fixed with 2.5% glutaraldehyde for 3 h at 8 °C, and post-fixed with 1% OsO_4 over night at 8 °C after twice washing with Milli-Q water. The supernatant was removed and the settled cells were transferred to a coverslip coated with poly-L-lysine (molecular weight 70,000–150,000). The attached cells were washed in Milli-Q water twice. The samples were then dehydrated in a series of ethanol (10, 30, 50, 70, 90 and 3 × in 100%, 10 min at each step), critical point dried (K850 Critical Point Dryer, Quorum/Emitech, West Sussex, UK), sputter-coated with gold, and examined with a Zeiss Sigma FE (Carl Zeiss Inc., Oberkochen, Germany) scanning electron microscope.

2.4. PCR amplifications and sequencing

The total *Azadinium poporum* DNA was extracted from 10 mL of exponentially growing cultures using a MiniBEST Universal DNA Extraction Kit (Takara, Tokyo, Japan) according to the manufacturer's protocol. PCR amplifications were carried out using 1 × PCR buffer, 50 µM dNTP mixture, 0.2 µM of each primer, 10 ng of template genomic DNA, and 1 U of ExTaq DNA Polymerase (Takara, Tokyo, Japan) in 50 µL reactions. The SSU rDNA was amplified using the primers PRIMERA/PRIMERB (Medlin et al., 1988). The LSU rDNA was amplified using the primers D1R/28-1483R (Scholin et al., 1994; Daugbjerg et al., 2000). The total ITS1–5.8S–ITS2 was amplified using ITSA/ITSB primers (Adachi et al., 1996). The thermal cycle procedure was 4 min at 94 °C, followed by 30 cycles of 1 min at 94 °C, 1 min at 45 °C, 1 min at 72 °C, and final extension of 7 min at 72 °C with a Mastercycler (Eppendorf, Hamburg, Germany). The PCR product was purified using a DNA purification kit (Shangong, Shanghai, China) and sequenced directly in both directions on an ABI PRISM 3730XL (Applied Biosystems, Foster City, CA, USA) following the manufacturer's instructions. Newly obtained sequences were deposited in the GenBank with accession numbers MH685461 to MH685468 (SSU rDNA), MH685480 to MH685495 (LSU rDNA) and MH685498 to MH685515 (ITS rDNA).

2.5. Sequence alignment and phylogenetic analysis

Newly obtained *Azadinium poporum* sequences (SSU, partial LSU and ITS rDNA) were incorporated into those of Amphidomataceae available in GenBank. Sequences were aligned using MAFFT v7.110 (Katoh and Standley, 2013) online program (http://mafft.cbrc.jp/alignment/server/). Alignments were manually checked with BioEdit v. 7.0.5 (Hall, 1999). For Bayesian inference (BI), the program jModelTest (Posada, 2008) was used to select the most appropriate model of molecular evolution with Akaike Information Criterion (AIC). Bayesian reconstruction of the data matrix was performed using MrBayes 3.2 (Ronquist and Huelsenbeck, 2003) with the best-fitting substitution model (GTR + G). Four Markov chain Monte Carlo (MCMC) chains ran for 5,000,000 generations, sampling every 100 generations. Convergence diagnostics were graphically estimated using "are we there yet" (http://ceb.scs.fsu.edu/awty) (Nylander et al., 2008) and the first 10% of burn-in trees were discarded. A majority rule consensus tree was created in order to examine the posterior probabilities of each clade. Maximum likelihood (ML) analyses were conducted with RaxML v7.2.6 (Stamatakis, 2006) on the T-REX web server (Boc et al., 2012) using the model GTR + G. Node support was assessed with 500 bootstrap replicates.

2.6. Chemical analysis of azaspiracids

Among 18 established strains of *A. poporum*, 15 cultures were able to be grown in 200 mL Erlenmeyer flasks under standard culture conditions. At exponential phase (determined using sequential cell counts) about 10^7 cells were collected by centrifugation. Exponential phase was determined via linear regression of log-transformed cell count time series. Cell pellets were extracted with 150 µL acetone by sonification with a sonotrode (Branson Sonifier) with 70% cycles at stage 2 for 1 min each. The extracts were then centrifuged (Eppendorf 5415 R, Hamburg, Germany) at 16,100 *g* at 4 °C for 10 min. Each supernatant was transferred to a 0.45 µm pore-size spin-filter (Millipore Ultrafree, Eschborn, Germany) and centrifuged for 30 s at 3000 *g*, and the resulting filtrate was transferred into a LC autosampler vial for LC–MS/MS analysis.

2.6.1. Single reaction monitoring (SRM) measurements

Water was deionized and purified (Milli-Q, Millipore, Eschborn, Germany) to 18 MΩ cm^{-1} or better quality. Formic acid (90%, p.a.), acetic acid (96%, p.a.) and ammonium formate (98%, p.a.) were from Merck (Darmstadt, Germany). The solvents, methanol and acetonitrile, were high performance liquid chromatography (HPLC) grade (Merck, Darmstadt, Germany).

Mass spectral experiments were performed to survey for a wide array of AZAs. The analytical system consisted of a triple quadrupole mass spectrometer (AB-SCIEX-4000 Q Trap, Darmstadt, Germany) equipped with a TurboSpray® interface coupled to HPLC (model 1100,Agilent, Waldbronn, Germany). The LC equipment included a solvent reservoir, in-line degasser (G1379A), binary pump (G1311A), refrigerated autosampler (G1329A/G1330B), and temperature-controlled column oven (G1316A).

Separation of AZA (5 µL sample injection volume) was performed by reverse-phase chromatography on a C8 phase. The analytical column (50 × 2 mm) was packed with 3 µm Hypersil BDS 120 Å (Phenomenex, Aschaffenburg, Germany) and maintained at 20 °C. The flow rate was 0.2 mL min^{-1} and gradient elution was performed with two eluants, wherein eluant A was water and B was acetonitrile/water (95:5 v/v), and both contained 2.0 mM ammonium formate and 50 mM formic acid. The initial conditions were 8 min column equilibration with 30% B, followed by a linear gradient to 100% B in 8 min, isocratic elution until 18 min with 100% B, and then returning to the initial conditions until 21 min (total run time: 29 min).

The AZA profiles were determined in one period (0–18 min) with curtain gas: 10 psi, CAD: medium, ion spray voltage: 5500 V, ambient temperature; nebulizer gas at 10 psi, auxiliary gas was off, the interface heater was on, the declustering potential @ 100 V, the entrance potential @ 10 V, and the exit potential @ 30 V. The SRM experiments were carried out in positive ion mode by selecting the transitions shown in Table 2. The AZA were calibrated against an external standard solution of AZA-2 (certified reference material programme of the IMB-NRC, Halifax, Canada) and expressed as AZA-2 equivalents.

2.6.2. Precursor ion experiments

Precursors of the fragments *m/z* 348, *m/z* 360 and *m/z* 362 were scanned in the positive ion mode from *m/z* 500 to 1000 under the following conditions: curtain gas at 10 psi, CAD at medium, ion spray voltage at 5500 V, ambient temperature, a 10 psi nebulizer gas, the auxiliary gas was off, the interface heater was on, a declustering potential of 100 V, a 10 V entrance potential, a 70 V collision energy, and a 12 V exit potential.

2.7. Effects of temperature on growth

Four strains were subjected to growth experiments, two (TIO420 and TIO424) representing ribotype A, and two (TIO429 and TIO452) representing ribotype C. Experiments on growth at various temperatures (11, 14, 17, 20, 23, 26, 29 and 32 °C) were conducted in triplicate using 200 mL glass bottles with 100 mL medium and an initial cell density of ~12,000 cells mL^{-1}. Healthy cultures were acclimated over a

Table 2
Mass transitions *m/z* (Q1 > Q3 mass) and their respective AZA.

Mass transition	Toxin	Collision energy (CE) [V]
716 > 698	AZA-33	40
796 > 778	AZA-33 phophate	40
816 > 798	AZA-34, AZA-39	40
816 > 348	AZA-39	70
828 > 658	AZA-3	70
828 > 810	AZA-3, AZA-43, AZA-58	40
830 > 812	AZA-38, AZA-52, AZA-53	40
830 > 348	AZA-38, AZA-52, AZA-53	70
842 > 672	AZA-1	70
842 > 824	AZA-1, AZA-40, AZA-50	40
842 > 348	AZA-40	70
844 > 826	AZA-4, AZA-5	40
846 > 828	AZA-37	40
846 > 348	AZA-37	70
854 > 836	AZA-41	40
854 > 670	AZA-41	70
854 > 360	AZA-41	70
856 > 672	AZA-2	70
856 > 838	AZA-2	40
858 > 840	AZA-7, AZA-8, AZA-9, AZA-10, AZA-36, AZA-51	40
858 > 348	AZA-36, AZA-51	70
860 > 842	AZA-59	40
868 > 362	AZA-55	70
870 > 852	Me-AZA-2, AZA-42, AZA-54	40
870 > 360	AZA-42	40
872 > 854	AZA-11, AZA-12	40
884 > 866	AZA-56	40
910 > 892	Undescribed	40
920 > 804	AZA-1 phosphate, AZA-40 phosphate	40
926 > 908	AZA-37 phosphate	40
936 > 918	AZA-2 phosphate	40
938 > 920	AZA-36 phosphate, AZA-51 phosphate	40
940 > 922	AZA-59 phosphate	40
952 > 938	AZA-11 phosphate	40

period of 15 days to low temperatures successively, at steps no greater than 3 °C at a time. The light: dark cycle in all experiments was 12:12 h. For sampling, 0.1 mL were removed from the culture at 3-day intervals and fixed in Lugol's solution. Each sample was transferred to a Sedgwick-Rafter chamber and a minimum of 200 cells per sample were counted.The specific growth rates in the exponential growth phase were calculated according to the method of Guillard (1973) by a least squares fit of a straight line to the data after logarithmic transformation.

3. Results

3.1. Morphology

Eighteen strains of *Azadinium poporum* were established by incubating sediments along the coast of Greece (Table 1). All strains were examined with LM and they were indistinguishable. The Greek *A. poporum* strain TIO420 (ribotype A) were 12.2–15.0 µm long (mean = 13.9 ± 0.6 µm, n = 30) and 9.3–11.4 µm wide (mean = 10.4 ± 0.5 µm, n = 30) with a median length: width ratio of 1.35. The cells had a conical epitheca and a hemispherical hypotheca (Fig. 1A–D). Up to three ring like pyrenoids were visible in the light microscope, and were located in the epitheca and/or in the hypotheca (Fig. 1A–D). The nucleus was large, spherical to slightly elongated and located in the cingular plane (Fig. 1E). Spherical or ellipsoid cysts were formed in cultures of strain TIO427 (Fig. 1F) with a diameter of 22.2–27.2 µm (mean = 25.2 ± 1.7 µm, n = 11). The cyst had a nucleus, contained many lipid globules, and lacked any obvious ornamentation visible with LM (Fig. 1G).

Under SEM, *A. poporum* strain TIO420 (ribotype A) showed a plate pattern of Po, cp, X, 4′, 3a, 6″, 6C, 5S, 6‴, 2⁗ (Fig. 2). The cingulum was deeply excavated and descended less than half of its width (Fig. 2A and B). The sulcus was composed of five sulcal plates, including an anterior sulcal (Sa), a median sulcal (Sm), a right sulcal (Sd), a left sulcal (Ss) and a posterior sulcal (Sp) plate (Fig. 2C). A round apical pore was located in the centre of the pore plate (Po) and was covered by a cover plate (cp) (Fig. 2D). There was a distinct ventral pore (vp) located at the junction of the pore plate and the first two apical plates (1′, 2′) (Fig. 2D). There were three anterior intercalary plates (1a, 2a and 3a) on the dorsal part of the epitheca (Fig. 2B, D and E). Plates 1a and 3a were much larger than the four-sided 2a plate (Fig. 2B, D and E). The first antapical plate (1⁗) was much smaller than the second antapical plate (2⁗) and displaced to the left (Fig. 2F). There was always a group of pores which typically consisted of 6–14 pores (mean = 8.6 ± 2.4, n = 9) located on the dorsal side of the second antapical plate (Fig. 2F). The cingulum comprised six plates of similar size (Fig. 2G).

Cells of the Greek *A. poporum* strain TIO429 (ribotype C) were 12.2–15.4 µm long (mean = 13.8 ± 0.9 µm, n = 30) and 8.9–11.8 µm wide (mean = 10.3 ± 0.9 µm, n = 30) with a median length: width ratio of 1.34. The cells of strain TIO429 shared identical morphology (Fig. 3) with strain TIO420, but the number of the distinct group of pores on the dorsal side of the second antapical plate was slightly larger (10–16, mean = 13 ± 2.4, n = 5) (Fig. 3D).

3.2. Molecular analysis and phylogeny

The ML and BI analysis based on concatenated SSU, partial LSU and ITS rDNA sequences yielded similar phylogenetic trees. The ML tree was illustrated in Fig. 4. Strains of *Azadinium poporum* from various parts of the world formed a well-resolved clade with maximal support (ML bootstrap support: 100/BI posterior probability: 1.0), comprising three well supported clades, referred as ribotypes A, B, and C. Twelve strains from Gulf of Amvrakikos and two strains from Gulf of Igoumenitsa fell within ribotype A, whereas four strains from Gulf of Igoumenitsa belonged to ribotype C (Fig. S1).

All Greek *A. poporum* strains shared nearly identical SSU rDNA sequences differing from each other only at one position. Strains of ribotype A shared identical LSU rDNA sequences and differed from each other only at 0 or 1 position in ITS rDNA sequences. Strains of ribotype C shared identical LSU rDNA sequences and differed from each other only at 0 to 2 positions in ITS rDNA sequences. Strains TIO420 (ribotype A) and TIO429 (ribotype C) shared 96.46% and 96.67% similarity in LSU and ITS rDNA sequences. Sequences similarity and genetic distances based on LSU and ITS rDNA sequences among *A. poporum* strains worldwide were listed in Tables 3 and 4.

Ribotypes A and C could be divided into two subclades respectively with maximal support. Ribotype A1 included strains from Denmark, Pacific USA, New Zealand and Chile, whereas ribotype A2 included strains from the Mediterranean Sea and French Atlantic. Ribotype C1 included strains from China, Korea and Argentina, whereas ribotype C2 included strains from the Mediterranean Sea and Gulf of Mexico.

3.3. AZA profiles

In seven out of 15 analysed *A. poporum* strains AZA could be detected. Among the AZA detected in the Greek strains were AZA-2, AZA-11, AZA-40 and AZA-59. In addition, the phosphorylated forms of AZA-2 and AZA-40 were found (Table 5). The most abundant AZA in all strains was AZA-40 that reached the highest cell quota of 30.2 fg cell^{-1} in strain TIO427 (Table 5). The second most abundant AZA was AZA-2 with up to 2.6 fg cell^{-1}, but for one of the three strains of ribotype C no AZA-2 was found. AZA-11 was only detected in strain TIO429 at a cell quota of 0.01 fg cell^{-1}. AZA-59 was also present at low levels up to 0.29 fg cell^{-1}. Phosphates typically were less than 1% of their respective parent compounds. The detection limits for the determination of AZA was calculated (signal-to-noise ratio S/N ≥ 3) between 0.001 and 0.01 fg cell^{-1} depending on available biomass of each strain.

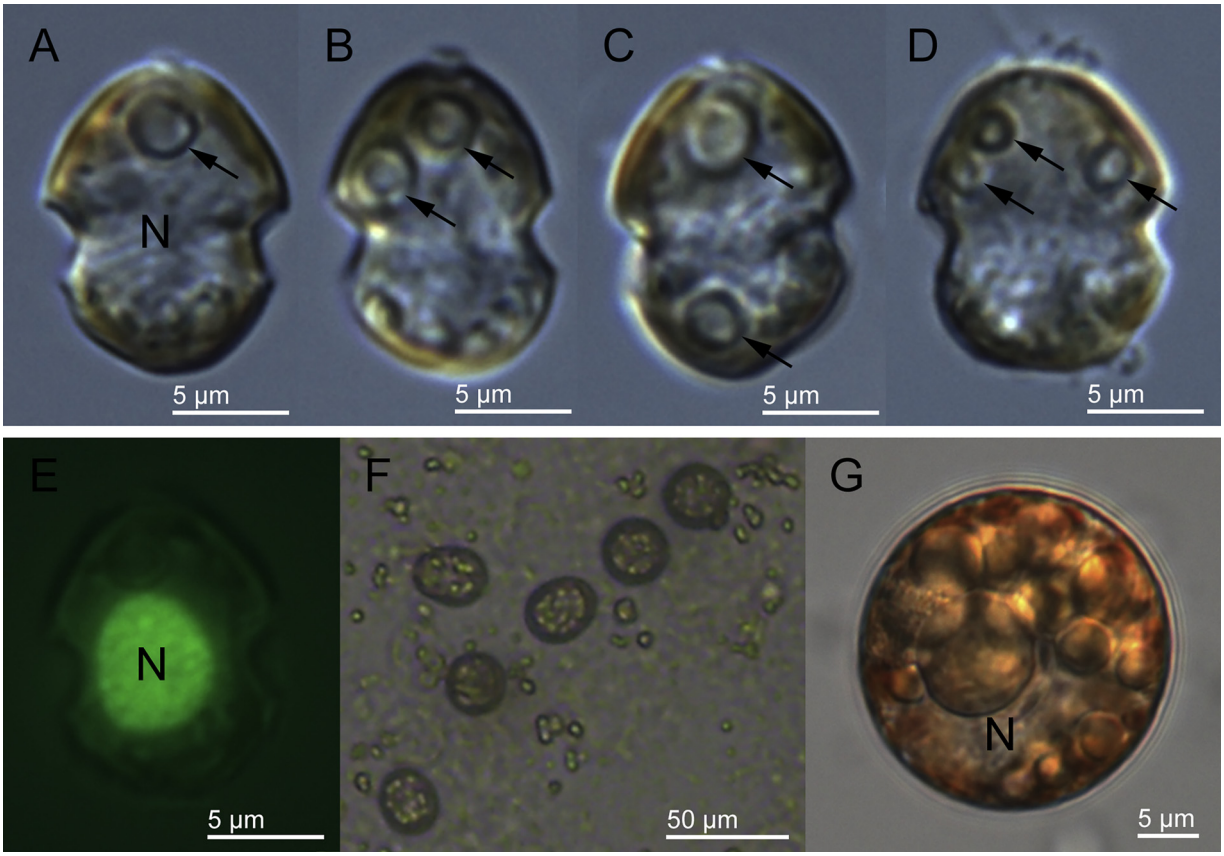

Fig. 1. LM of live cells (strain TIO420) and cysts (strain TIO427) of *Azadinium poporum*. (A–D) Ventral view showing a conical epitheca and a round hypotheca with variable number of pyrenoids (arrows). (E) A SYBR Green-stained cell, showing the large nucleus (N). (F) Spherical and ellipsoidal cysts formed in culture. (G) A spherical cyst, showing many granules and a nucleus (N) (For interpretation of the references to colour in this figure legend, the reader is referred to the web version of this article).

All Greek strains without detectable AZA belonged to the *A. poporum* ribotype A, However, four out of the twelve strains of ribotype A produced low levels of AZA-2 and AZA-40, which did not exceed a total AZA cell quota of 0.07 fg cell^{-1}.

3.4. Effects of temperature on growth

Strains TIO420 and TIO424 of ribotype A exhibited growth at temperatures between 11 and 26 °C. The highest division rate was around 0.3 divisions d^{-1} at 14 °C for strain TIO420 (0.4 divisions d^{-1} at 23 °C for strain TIO424), and then dropped slowly towards higher and lower temperatures.

Strain TIO429 of ribotype C exhibited growth at temperatures between 11 and 32 °C. Exponential division rates were similar at temperature from 17 to 32 °C (around 0.5 divisions d^{-1}) and much higher than those at 11 and 14 °C (< 0.3 divisions d^{-1}). Strain TIO452 of ribotype C exhibited growth at temperatures between 17 and 32 °C. The highest division rate was around 0.4 divisions d^{-1} at 32 °C and then dropped slowly towards lower temperatures (Fig. 5).

4. Discussion

4.1. Morphology and biogeography of A. poporum

In previous surveys on harmful dinoflagellates, *Azadinium* like cells were not reported in Greek waters including Ionian Sea (Ignatiades and Gotsis-Skretas, 2010). They were probably missed as *Azadinium* was not identified until 2009 (Tillmann et al., 2009). AZA-1, AZA-2 and AZA-3 were not detected in a previous survey on mussels from Northern Aegean Sea either (Ciminiello et al., 2006), but the lack of AZA in shellfish probably is due to the fact that other AZA such as AZA-40 were not analyzed.

The new *Azadinium poporum* strains from Ionian Sea of Mediterranean Sea fit the original descriptions in all aspects including the number and configuration of apical and anterior intercalary plates and a prominent ventral pore at the left side of apical pore complex (Tillmann et al., 2011). Previsouly *Azadinium poporum* has not been reported in Greek waters and thus is the first record here. The two strains of different ribotypes examined in detail (TIO420 and TIO429) are indistinguishable morphologically. The number of the group of pores in the second antapical plate for the two strains are slightly different, but the number of grouped pores on the second antapical plate has been reported to vary from a few to numerous in a clonal Chilean strain (Tillmann et al., 2017b). This feature thus seems to be of little diagnostic values. Occurrence of *Azadinium poporum* has been reported from the North Sea, from East Asia, New Zealand, Argentina, Chile, from the Gulf of Mexico, Western Mediterranean Sea, French Atlantic and Pacific USA (Potvin et al., 2011; Tillmann et al., 2011; Gu et al., 2013; Smith et al., 2016; Luo et al., 2016; Tillmann et al., 2016; Kim et al., 2017; Luo et al., 2017a; Tillmann et al., 2017b). Here its distribution is extended to the Eastern Mediterranean Sea for the first time, further supporting the view that *A. poporum* is a widely distributed species.

All *A. poporum* strains examined here originated from surface sediments incubation, supporting the view that cyst stages must be present in this species. Spherical and ellipsoid cysts of *A. poporum* ribotype B have been reported in culture previously (Gu et al., 2013) and much smaller (15 µm vs 25 µm) than cysts produced by *A. poporum* ribotype C as reported here. However, nothing is known about the type and functional role of these cysts and direct observations on cyst formation

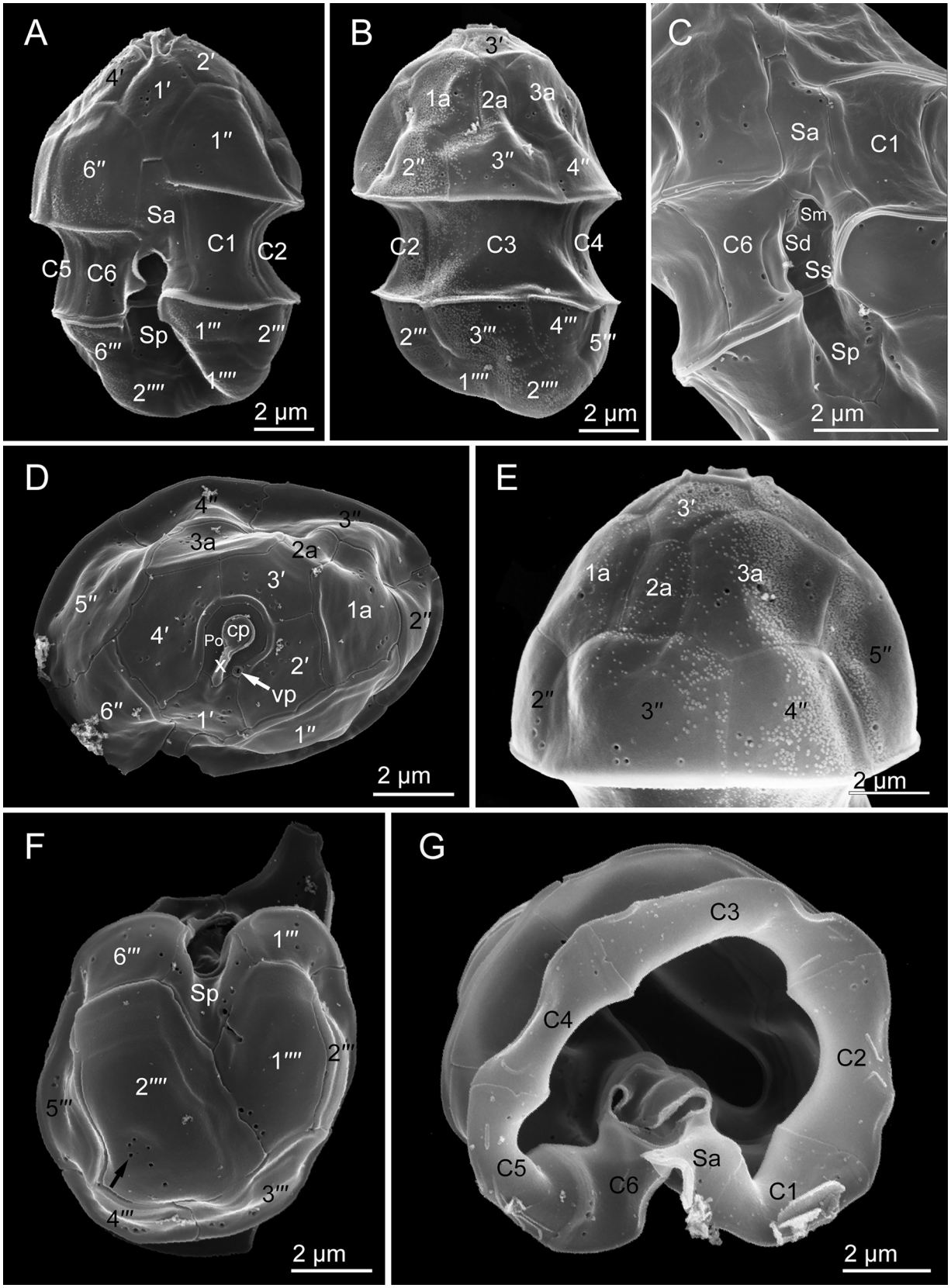

Fig. 2. Scanning electron micrographs of vegetative cells of *Azadinium poporum* strain TIO420. (A) Ventral view showing the first apical plate (1′) and cingulum displacement. (B) Dorsal view showing three anterior intercalary plates (1a, 2a and 3a) and three of the cingular plates (C2, C3 and C4). (C) Sulcal plates showing an anterior sulcal plate (Sa), a median sulcal plate (Sm), a right sulcal plate (Sd), a left sulcal plate (Ss), and a posterior sulcal plate (Sp). (D) Apical view showing four apical plates (1′ – 4′), six precingular plates (1″ – 6″), a pore plate (Po), a cover plate (cp), a canal plate (X), and a ventral pore (vp). (E) Dorsal view, showing three anterior intercalary plates (1a, 2a, and 3a). (F) Antapical view showing six postcingular plates (1‴ – 6‴), two antapical plates (1⁗, 2⁗) of unequal size and a group of pores on the dorsal side of plate 2⁗ (arrow). (G). The cingulum showing six cingular plates of similar size.

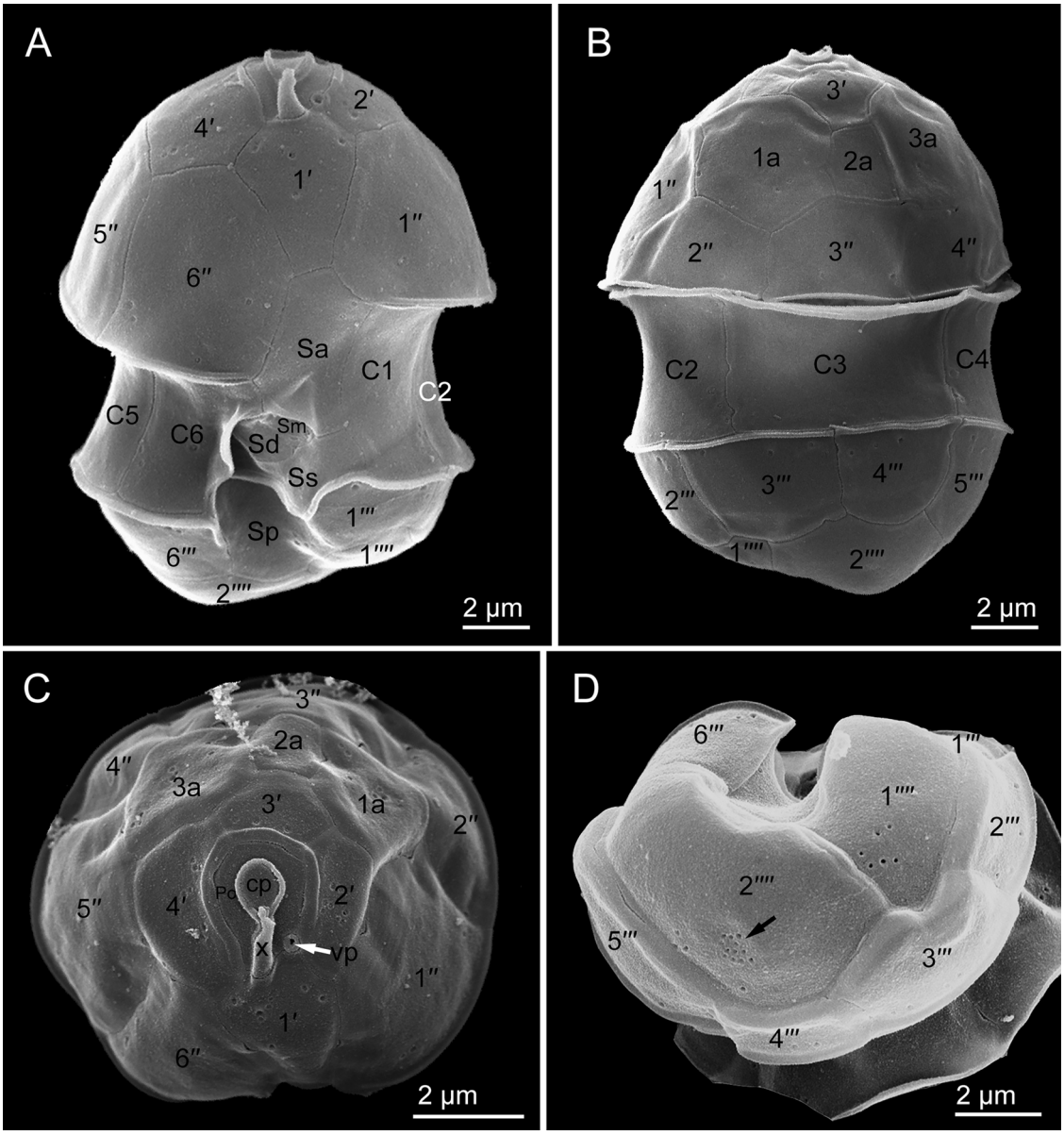

Fig. 3. Scanning electron micrographs of vegetative cells of *Azadinium poporum* strain TIO429. (A) Ventral view showing the first apical plate (1′), an anterior sulcal plate (Sa), a median sulcal plate (Sm), a right sulcal plate (Sd), a left sulcal plate (Ss), and a posterior sulcal plate (Sp). (B) Dorsal view showing three anterior intercalary plates (1a, 2a and 3a) and three cingular plates (C2, C3 and C4). (C) Apical view showing four apical plates (1′ – 4′), six precingular plates (1″ – 6″), a pore plate (Po), a cover plate (cp), a canal plate (X), and a ventral pore (vp). (D) Antapical view showing six postcingular plates (1‴ – 6‴), two antapical plates (1⁗, 2⁗) of unequal size and a group of pores on the dorsal side of plate 2⁗.

and hatching are missing yet. Despite continuous attempts, identification of *Azadinium* cysts similar to the ones observed in cultures in the Greek sediments failed. These cysts probably are too small and inconspicuous thus escaping our detection, or the cysts in the field might be completely different from those in culture.

4.2. Genetic differentiation among A. poporum strains

With the availability of multiple strains, substantial genetic differentiations within species of *Azadinium* become more and more evident. New strains from the French Atlantic and from the Salish Sea (North America) revealed substantial sequence variability among *A. dalianense* strains from different areas (Kim et al., 2017; Luo et al., 2017a). For *A. poporum*, genetic differentiation of strains has been repeatedly reported and so far three ribotypes have been identified (Gu et al., 2013). Our results support and strengthen the idea that there are further levels of genetic differentiation within ribotype A (referred as A1 and A2 in Fig. 4) (Luo et al., 2017a) and demonstrate that genetic differences also exist within ribotype C (referred as C1 and C2 in Fig. 4).

Two ribotypes of *A. poporum* have been reported in Chinese coast, with ribotypes B and C co-occurring in the East China Sea and South China Sea (Gu et al., 2013). Sympatric occurrence of ribotypes A and C has not been recorded before, but is shown here for the first time for the Eastern Mediterranean Sea. Ribotype A was recorded in Western Mediterranean Sea, but at that time only one strain was available for sequencing (Luo et al., 2017a), and a large number of strains are necessary to uncover a potential presence of additional ribotypes. The genetic distances among *A. poporum* strains based on ITS rDNA sequences could reach as much as 0.035, close to a threshold value of 0.04 that typically differentiate dinoflagellates at an interspecific level (Litaker et al., 2007). Among all three *A. poporum* ribotypes, however, compensatory based changes within helix III of ITS rDNA were not

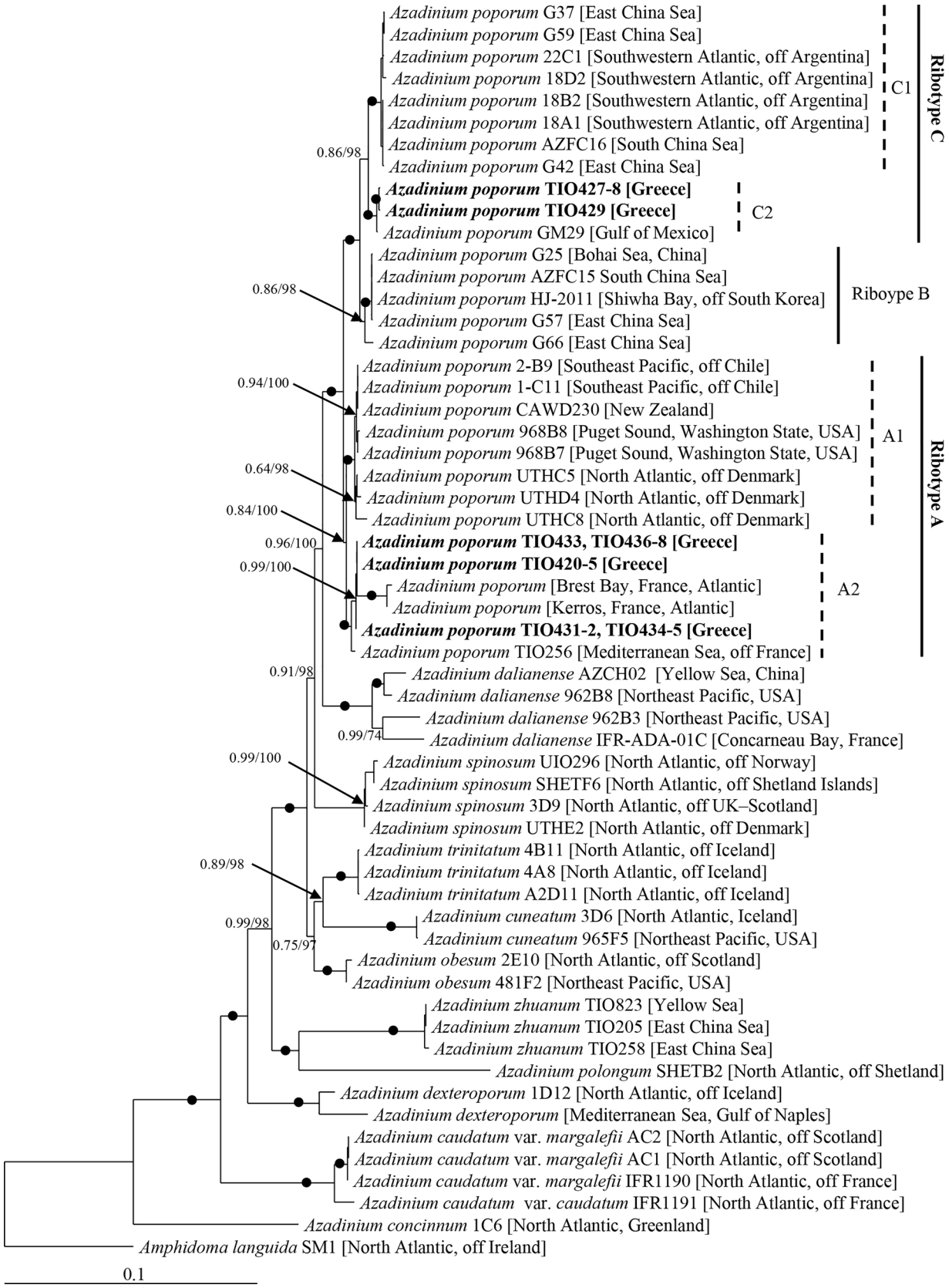

Fig. 4. Phylogeny of *Azadinium poporum* inferred from concatenated SSU, partial LSU and ITS rDNA sequences using Maximum likelihood (ML). New sequences are indicated in bold. Branch lengths are drawn to scale, with the scale bar indicating the number of nucleotide substitutions per site. Numbers on branches are statistical support values to clusters on the right of them (left: Bayesian posterior probabilities; right: ML bootstrap support values). Black dots indicate maximal support (BPP = 1.00 and ML BS = 100).

Table 3
LSU rDNA sequences comparison of *Azadinium poporum* from representative areas. The percentage (%) above the diagonal line refers to the similarity out of partial LSU rDNA sequences; the numeral below the diagonal line refers to pairwise genetic distance. (1: Greece, ribotype A; 2: Denmark, ribotype A; 3: Corsica, ribotype A; 4: French Atlantic, ribotype A; 5: French Atlantic, ribotype A; 6: USA Pacific, ribotype A; 7: New Zealand, ribotype A; 8: Chile, ribotype A; 9: Bohai Sea, ribotype B; 10: East China Sea, ribotype C; 11: Argentina, ribotype C; 12: Gulf of Mexico, ribotype C; 13: Greece, ribotype C).

	TIO420	UTHC8	TIO256	10-117	10-269	967B8	CAWD230	2b9	G25	G42	22C1	GM29	TIO429
TIO420[1]	–	98.46	99.54	100	100	98.46	98.46	98.46	96.46	97.23	96.92	96.46	96.46
UTHC8[2]	0.015	–	98.31	98.46	98.46	99.54	99.85	99.85	95.99	96.30	95.99	95.07	95.07
TIO256[3]	0.005	0.017	–	99.54	99.54	98.31	98.31	98.31	96.61	97.07	97.07	96.30	96.30
10–117[4]	0.000	0.015	0.005	–	100	98.46	98.46	98.46	96.46	97.23	96.92	96.46	96.46
10–269[5]	0.000	0.015	0.005	0.000	–	98.46	98.46	98.46	96.46	97.23	96.92	96.46	96.46
967B8[6]	0.015	0.005	0.017	0.015	0.015	–	99.54	99.54	95.84	96.30	96.15	95.07	95.07
CAWD230[7]	0.015	0.002	0.017	0.015	0.015	0.005	–	100	95.99	96.30	95.99	95.07	95.07
2b9[8]	0.015	0.002	0.017	0.015	0.015	0.005	0.000	–	95.99	96.30	95.99	95.07	95.07
G25[9]	0.034	0.039	0.032	0.034	0.034	0.040	0.039	0.039	–	97.38	97.38	97.38	97.38
G42[10]	0.026	0.036	0.028	0.026	0.026	0.036	0.036	0.036	0.025	–	99.54	98.00	98.00
22C1[11]	0.029	0.039	0.028	0.029	0.029	0.037	0.039	0.039	0.025	0.003	–	98.00	98.00
GM29[12]	0.034	0.048	0.036	0.034	0.034	0.048	0.048	0.048	0.025	0.019	0.019	–	100
TIO429[13]	0.034	0.048	0.036	0.034	0.034	0.048	0.048	0.048	0.025	0.019	0.019	0.000	–

Table 4
ITS rDNA sequences comparison of *Azadinium poporum* from representative areas. The percentage (%) above the diagonal line refers to the similarity out of ITS rDNA sequences; the numeral below the diagonal line refers to pairwise genetic distance based on ITS rDNA sequences. (1: Greece, ribotype A; 2: Denmark, ribotype A; 3: Corsica, ribotype A; 4: USA Pacific, ribotype A; 5: Chile, ribotype A; 6: Bohai Sea, ribotype B; 7: East China Sea, ribotype C; 8: Argentina, ribotype C; 9: Gulf of Mexico, ribotype C; 10: Greece, ribotype C).

	TIO420	UTHC8	TIO256	967B8	2b9	G25	G42	22C1	GM29	TIO429
TIO420[1]	–	98.17	99.00	98.00	98.33	96.50	96.00	96.00	97.00	96.67
UTHC8[2]	0.017	–	98.33	99.50	99.50	97.33	97.33	97.33	97.67	97.00
TIO256[3]	0.010	0.015	–	98.17	98.50	96.83	96.50	96.50	97.33	96.67
967B8[4]	0.020	0.003	0.018	–	99.67	97.33	97.33	97.33	97.67	97.00
2b9[5]	0.017	0.003	0.015	0.003	–	97.33	97.33	97.33	98.00	97.33
G25[6]	0.030	0.020	0.027	0.022	0.022	–	97.67	97.67	98.33	98.00
G42[7]	0.035	0.020	0.030	0.022	0.022	0.018	–	99.17	97.83	97.50
22C1[8]	0.035	0.020	0.030	0.022	0.022	0.018	0.003	–	97.83	97.50
GM29[9]	0.025	0.017	0.022	0.018	0.015	0.012	0.017	0.017	–	98.83
TIO429[10]	0.029	0.024	0.029	0.025	0.022	0.015	0.020	0.020	0.000	–

Table 5
Azaspiracid profiles of *Azadinium poporum* examined in the present study (na = not analyzed; nd = not detected; P = phosphate).

Species	Strains	Ribotypes	AZA	AZA-40 (fg cell^{-1})	AZA-40 P (fg cell^{-1})	AZA-2 (fg cell^{-1})	AZA-2 P (fg cell^{-1})	AZA-11 (fg cell^{-1})	AZA-59 (fg cell^{-1})
Azadinium poporum	TIO420	A	None	nd	nd	nd	nd	nd	nd
Azadinium poporum	TIO421	A	None	nd	nd	nd	nd	nd	nd
Azadinium poporum	TIO422	A	None	nd	nd	nd	nd	nd	nd
Azadinium poporum	TIO423	A	None	nd	nd	nd	nd	nd	nd
Azadinium poporum	TIO424	A	None	nd	nd	nd	nd	nd	nd
Azadinium poporum	TIO425	A	None	nd	nd	nd	nd	nd	nd
Azadinium poporum	TIO433	A	na	–	–	–	–	–	–
Azadinium poporum	TIO434	A	na	–	–	–	–	–	–
Azadinium poporum	TIO435	A	None	nd	nd	nd	nd	nd	nd
Azadinium poporum	TIO436	A	Present	0.01	nd	0.01	nd	nd	nd
Azadinium poporum	TIO437	A	Present	0.06	nd	nd	nd	nd	nd
Azadinium poporum	TIO438	A	Present	0.01	nd	nd	nd	nd	nd
Azadinium poporum	TIO431	A	Present	0.06	nd	0.01	nd	nd	nd
Azadinium poporum	TIO432	A	None	nd	nd	nd	nd	nd	nd
Azadinium poporum	TIO427	C	Present	30.2	0.09	nd	nd	nd	0.29
Azadinium poporum	TIO428	C	Present	16.5	0.03	2.6	0.002	nd	0.08
Azadinium poporum	TIO429	C	Present	9.6	0.08	2.1	0.01	0.01	0.04
Azadinium poporum	TIO452	C	na	–	–	–	–	–	–

found (Gu et al., 2013), suggesting that cryptic speciation has not occurred in *A. poporum* yet.

Genetic differentiation of dinoflagellates is often related with geographic separation and limited gene flow (Kim et al., 2004; Penna et al., 2005; Al-Kandari et al., 2011). Sympatric distribution of various ribotypes is not common in dinoflagellates and is reported in only a few species, e.g. *Scrippsiella acuminata* (Montresor et al., 2003), *Akashiwo sanguinea* (Luo et al., 2017b) and *Peridinium cinctum* (Izquierdo López et al., 2017). A correlation between ribotype and physiology has been reported in *Akashiwo sanguinea* where ribotype A blooms in winter and spring but ribotype B blooms in summer (Luo et al., 2017b). Likewise, Greek *A. poporum* strains of various ribotypes differ in their AZA production potential. Levels of AZA of ribotype A from Greece strains were very low or below detection limit, but Greek strains of ribotype C produces high levels of different AZA. In addition, Greek ribotype A strains grow better at high temperature (Table S1). This indicates a potential niche separation between both ribotypes, but any differentiated seasonal occurrence in the field remains to be determined.

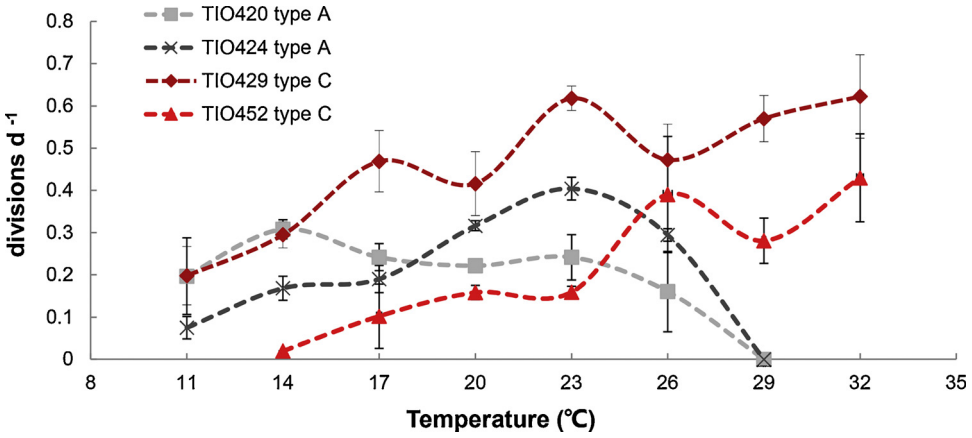

Fig. 5. Growth responses of four strains of *Azadinium poporum* ribotypes A and C under various temperatures.

The high genetic differentiation among sympatric *A. poporum* strains in the Eastern Mediterranean Sea is in contrast to the fact that *A. poporum* strains from distant areas share identical sequences. For example, *A. poporum* strains from Denmark and New Zealand share identical LSU rDNA sequences (Smith et al., 2016) and Greek *A. poporum* ribotype C share identical LSU rDNA sequences with that of Gulf of Mexico strain (Luo et al., 2016). This might be explained by recent dispersal through ballast water, which is especially possible for species with a cyst stage (Hallegraeff, 1998). In contrast, the occurrence of *A. poporum* ribotype A2 in French Atlantic, Western Mediterranean Sea and Eastern Mediterranean Sea might be explained by natural dispersal due to the eastward surface water flow from Atlantic across the Mediterranean Sea (Pinet, 2009). The high variability of LSU rDNA sequences challenges the rapid detection of *A. poporum* using the FISH probe and qPCR designed based on the few Danish strains available at that time (Toebe et al., 2013). These published qPCR primers do not absolutely match sequences of the new Greek strains, differing at one or two positions, and the TaqMan MGB probe (Toebe et al., 2013) differ from strains TIO420 and TIO429 at 3 and 6 positions. Based on this data new primers and probes need to be designed in order to comprehensively detect all now known *A. poporum* strains.

4.3. AZA profiles of Greek A. poporum

The Greek strains of *A. poporum* produced four AZA variants (AZA-2, AZA-11, AZA-40 and AZA-59), with AZA-40 and AZA -2 consistently being the most abundant compounds of the AZA-positive strains. It is, however, interesting to note that one ribotype C strain lack any detectable amounts of AZA-2. Such a variability of toxin profile among strains from the same area was recorded before only from Chinese waters (Krock et al., 2014). Among the AZA congeners, the respective phosphates of AZA-40 and AZA-2 were also detected, at least in some cases. The fact that no AZA-11 and -59 phosphate was detected in the Greek *A. poporum* strains is probably due to the fact that these AZA were only produced at low amounts at cell quotas < 0.1 fg cell^{-1} so that the phosphate forms, which usually make up only 1% of the parent compound, would not be detectable. The production of low amounts of AZA phosphates in comparison to their parent compounds has recently been described for *A. poporum* from the Southwest Atlantic (Tillmann et al., 2016) and the Southeast Pacific (Tillmann et al., 2017b) and seems to be a general trait of *A. poporum*.

AZA-2 is the most widespread AZA and is found in *A. spinosum*, *A. poporum* and *Amphidoma languida* (Tillmann et al., 2009; Krock et al., 2014; Tillmann et al., 2017a). In *A. poporum* strains it was reported from the Gulf of Mexico (Luo et al., 2016), the South Atlantic (Tillmann et al., 2016), the Northwest Pacific (Krock et al., 2014), the Southwest Pacific (Tillmann et al., 2017b), and recently also from the ribotype A strain from Corsica, Mediterranean (Luo et al., 2017a). Another AZA produced by Greek strains, AZA-11, has up to now been reported from the Pacific region (China and Chile) (Krock et al., 2014; Tillmann et al., 2017b). AZA-11 was found in all three ribotypes, being recorded in Chinese ribotype B and C strains (Gu et al., 2013) and in Chilean ribotype A strains (Tillmann et al., 2017b). In contrast, AZA-40 and AZA-59 are currently known from just a few areas, i.e AZA-40 was reported from the China Sea (Krock et al., 2014), and AZA-59 very recently from coastal water of Washington State, USA (Kim et al., 2017). The current finding of AZA-40 and AZA-59 (albeit in low amounts) also in the Eastern Mediterranean clearly show that a wide geographical distribution might be a common feature for all AZA congeners. This is likely to become more evident in the future when updated AZA analysis including the whole suite of newly detected compounds is increasingly applied for more field samples and strains.

Of the four AZA variants detected in *A. poporum* strains from the Eastern Mediterranean Sea, only AZA-2 is included in European food safety regulations. The fact that AZA-40 (not regulated) in the Greek strains is approximately one order of magnitude more abundant than AZA-2 (regulated) underlines that current monitoring strategies underestimate of total AZA load and consequently the risk of Azaspiracid Shellfish Poisoning (AZP) events in Greek waters. However, for a full risk assessment, detailed data on specific toxicity of AZA-40 are needed.

Acknowledgements

We thank Thomas Max for technical assistance with toxin extraction and measurements and P. Drakopoulou for making the Fig. S1. This work was supported by the National Key Research and Development Program of China (2016YFE0202100), National Natural Science Foundation of China (41676117), Bilateral International Cooperation Fund of State Oceanic Administration. The work was partially funded by the Helmholtz-Gemeinschaft Deutscher Forschungszentren through the research program PACES of the Alfred Wegener Institut-Helmholtz Zentrum für Polar- und Meeresforschung and the BMBF project RIPAZA (grant nr 03F0763A). [SS]

Appendix A. Supplementary data

Supplementary material related to this article can be found, in the online version, at doi:https://doi.org/10.1016/j.hal.2018.08.003.

References

Adachi, M., Sako, Y., Ishida, Y., 1996. Analysis of *Alexandrium* (Dinophyceae) species using sequences of the 5.8S ribosomal DNA and internal transcribed spacer regions. J. Phycol. 32 (3), 424–432.

Al-Kandari, M.A., Highfield, A.C., Hall, M.J., Hayes, P., Schroeder, D.C., 2011. Molecular

tools separate harmful algal bloom species, *Karenia mikimotoi*, from different geographical regions into distinct sub-groups. Harmful Algae 10 (6), 636–643.
Bacchiocchi, S., Siracusa, M., Ruzzi, A., Gorbi, S., Ercolessi, M., Cosentino, M.A., Ammazzalorso, P., Orletti, R., 2015. Two-year study of lipophilic marine toxin profile in mussels of the North-central Adriatic Sea: first report of azaspiracids in Mediterranean seafood. Toxicon 108, 115–125.
Beza, E.P., Kitsantas, D.T., Mitselos, A.F., 2014. Ship waste management in the port of Igoumenitsa Greece. J. Phys. Sci. Appl. 4 (6), 375–380.
Boc, A., Diallo, A.B., Makarenkov, V., 2012. T-REX: a web server for inferring, validating and visualizing phylogenetic trees and networks. Nucleic Acids Res. 40 (W1), W573–W579.
Busch, J.A., Andree, K.B., Diogène, J., Fernández-Tejedor, M., Toebe, K., John, U., Krock, B., Tillmann, U., Cembella, A.D., 2016. Toxigenic algae and associated phycotoxins in two coastal embayments in the Ebro Delta (NW Mediterranean). Harmful Algae 55, 191–201.
Ciminiello, P., Dell'Aversano, C., Fattorusso, E., Forino, M., Magno, S., Santelia, F., Tsoukatou, M., 2006. Investigation of the toxin profile of Greek mussels *Mytilus galloprovincialis* by liquid chromatography—mass spectrometry. Toxicon 47 (2), 174–181.
Daugbjerg, N., Hansen, G., Larsen, J., Moestrup, Ø., 2000. Phylogeny of some of the major genera of dinoflagellates based on ultrastructure and partial LSU rDNA sequence data, including the erection of three new genera of unarmoured dinoflagellates. Phycologia 39 (4), 302–317.
Gu, H., Luo, Z., Krock, B., Witt, M., Tillmann, U., 2013. Morphology, phylogeny and azaspiracid profile of *Azadinium poporum* (Dinophyceae) from the China Sea. Harmful Algae 21–22, 64–75.
Guillard, R.R.L., 1973. Division rates. In: Stein, J.R. (Ed.), Handbook of Phycological Methods. Culture Methods and Growth Measurements. Cambridge University Press, Cambridge, New York, pp. 289–311.
Guillard, R.R.L., Ryther, J.H., 1962. Studies of marine planktonic diatoms. I. *Cyclotella nana* Hustedt and *Detonula confervacea* Cleve. Can. J. Microbiol. 8, 229–239.
Hall, T.A., 1999. BioEdit: A User-friendly Biological Sequence Alignment Editor and Analysis Program for Windows 95/98/NT. pp. 95–98.
Hallegraeff, G.M., 1998. Transport of toxic dinoflagellates via ships' ballast water: bioeconomic risk assessment and efficacy of possible ballast water management strategies. Mar. Ecol. Prog. Ser. 168 (1), 297–309.
Ignatiades, L., Gotsis-Skretas, O., 2010. A review on toxic and harmful algae in Greek coastal waters (E. Mediterranean Sea). Toxins 2 (5), 1019–1037.
Izquierdo López, A., Kretschmann, J., Žerdoner Čalasan, A., Gottschling, M., 2017. The many faces of *Peridinium cinctum* (Peridiniaceae, Peridiniales): morphological and molecular variability in a common dinophyte. Eur. J. Phycol. 1–10.
Katoh, K., Standley, D.M., 2013. MAFFT multiple sequence alignment software version 7: improvements in performance and usability. Mol. Biol. Evol. 30 (4), 772–780.
Kehayias, G., Aposporis, M., 2014. Zooplankton variation in relation to hydrology in an enclosed hypoxic bay (Amvrakikos Gulf, Greece). Mediterr. Mar. Sci. 15 (3), 554–568.
Kim, E., Wilcox, L., Graham, L., Graham, J., 2004. Genetically distinct populations of the dinoflagellate *Peridinium limbatum* in neighboring Northern Wisconsin lakes. Microb. Ecol. 48 (4), 521–527.
Kim, J.-H., Tillmann, U., Adams, N.G., Krock, B., Stutts, W.L., Deeds, J.R., Han, M.-S., Trainer, V.L., 2017. Identification of *Azadinium* species and a new azaspiracid from *Azadinium poporum* in Puget Sound, Washington State, USA. Harmful Algae 68, 152–167.
Krock, B., Tillmann, U., Voß, D., Koch, B.P., Salas, R., Witt, M., Potvin, É., Jeong, H.J., 2012. New azaspiracids in Amphidomataceae (Dinophyceae). Toxicon 60 (5), 830–839.
Krock, B., Tillmann, U., Witt, M., Gu, H., 2014. Azaspiracid variability of *Azadinium poporum* (Dinophyceae) from the China Sea. Harmful Algae 36, 22–28.
Litaker, W.R., Vandersea, M.W., Kibler, S.R., Reece, K.S., Stokes, N.A., Lutzoni, F.M., Yonish, B.A., West, M.A., Black, M.N.D., Tester, P.A., 2007. Recognizing dinoflagellate species using ITS rDNA sequences. J. Phycol. 43 (2), 344–355.
Luo, Z., Gu, H., Krock, B., Tillmann, U., 2013. *Azadinium dalianense*, a new dinoflagellate species from the Yellow Sea, China. Phycologia 52 (6), 625–636.
Luo, Z., Krock, B., Mertens, K.N., Price, A.M., Turner, R.E., Rabalais, N.N., Gu, H., 2016. Morphology, molecular phylogeny and azaspiracid profile of *Azadinium poporum* (Dinophyceae) from the Gulf of Mexico. Harmful Algae 55, 56–65.
Luo, Z., Krock, B., Mertens, K.N., Nézan, E., Chomérat, N., Bilien, G., Tillmann, U., Gu, H., 2017a. Adding new pieces to the *Azadinium* (Dinophyceae) diversity and biogeography puzzle: non-toxigenic *Azadinium zhuanum* sp. nov. from China, toxigenic *A. poporum* from the Mediterranean, and a non-toxigenic *A. dalianense* from the French Atlantic. Harmful Algae 66, 65–78.
Luo, Z., Yang, W., Leaw, C.P., Pospelova, V., Bilien, G., Liow, G.R., Lim, P.T., Gu, H., 2017b. Cryptic diversity within the harmful dinoflagellate *Akashiwo sanguinea* in coastal Chinese waters is related to differentiated ecological niches. Harmful Algae 66, 88–96.
Medlin, L., Elwood, H.J., Stickel, S., Sogin, M.L., 1988. The characterization of enzymatically amplified eukaryotic 16S-like rRNA-coding regions. Gene 71 (2), 491–499.
Montresor, M., Sgrosso, S., Procaccini, G., Kooistra, W.H.C.F., 2003. Intraspecific diversity in *Scrippsiella trochoidea* (Dinopbyceae): evidence for cryptic species. Phycologia 42 (1), 56–70.
Naeher, S., Geraga, M., Papatheodorou, G., Ferentinos, G., Kaberi, E., Schubert, C.J., 2012. Environmental variations in a semi-enclosed embayment (Amvrakikos Gulf, Greece) – reconstructions based on benthic foraminifera abundance and lipid biomarker pattern. Biogeosciences 9, 7405–7441.
Nylander, J.A., Wilgenbusch, J.C., Warren, D.L., Swofford, D.L., 2008. AWTY (are we there yet?): a system for graphical exploration of MCMC convergence in Bayesian phylogenetics. Bioinformatics 24 (4), 581–583.
Penna, A., Vila, M., Fraga, S., Giacobbe, M.G., Andreoni, F., Riobó, P., Vernesi, C., 2005. Characterization of *Ostreopsis* and *Coolia* (Dinophyceae) isolates in the Western Mediterranean sea based on morphology, toxicity and Internal Transcribed Spacer 5.8 S rDNA sequences. J. Phycol. 41 (1), 212–225.
Percopo, I., Siano, R., Rossi, R., Soprano, V., Sarno, D., Zingone, A., 2013. A new potentially toxic *Azadinium* species (Dinophyceae) from the Mediterranean Sea, *A. dexteroporum* sp. nov. J. Phycol. 49 (5), 950–966.
Pinet, P.R., 2009. Invitation to Oceanography, 5th ed. Jones & Bartlett, Sudbury, Ontario, Canada.
Posada, D., 2008. jModelTest: phylogenetic model averaging. Mol. Biol. Evol. 25 (7), 1253–1256.
Potvin, É., Jeong, H.J., Kang, N.S., Tillmann, U., Krock, B., 2011. First report of the photosynthetic dinoflagellate genus *Azadinium* in the Pacific Ocean: morphology and molecular characterization of *Azadinium* cf. *poporum*. J. Eukaryot. Microbiol. 59, 145–156.
Ronquist, F., Huelsenbeck, J.P., 2003. MrBayes 3: Bayesian phylogenetic inference under mixed models. Bioinformatics 19 (12), 1572–1574.
Rossi, R., Dell'Aversano, C., Krock, B., Ciminiello, P., Percopo, I., Tillmann, U., Soprano, V., Zingone, A., 2017. Mediterranean *Azadinium dexteroporum* (Dinophyceae) produces six novel azaspiracids and azaspiracid-35: a structural study by a multi-platform mass spectrometry approach. Anal. Bioanal. Chem. 409 (4), 1121–1134.
Scholin, C.A., Herzog, M., Sogin, M., Anderson, D.M., 1994. Identification of group- and strain-specific genetic markers for globally distributed *Alexandrium* (Dinophyceae). II. Sequence analysis of a fragment of the LSU rRNA gene. J. Phycol. 30 (6), 999–1011.
Smith, K.F., Rhodes, L., Harwood, D.T., Adamson, J., Moisan, C., Munday, R., Tillmann, U., 2016. Detection of *Azadinium poporum* in New Zealand: the use of molecular tools to assist with species isolations. J. Appl. Phycol. 28, 1125–1132.
Stamatakis, A., 2006. RAxML-VI-HPC: maximum likelihood-based phylogenetic analyses with thousands of taxa and mixed models. Bioinformatics 22 (21), 2688–2690.
Tillmann, U., Elbrächter, M., Krock, B., John, U., Cembella, A., 2009. *Azadinium spinosum* gen. et sp. nov. (Dinophyceae) identified as a primary producer of azaspiracid toxins. Eur. J. Phycol. 44 (1), 63–79.
Tillmann, U., Elbrächter, M., John, U., Krock, B., 2011. A new non-toxic species in the dinoflagellate genus *Azadinium*: *A. poporum* sp. nov. Eur. J. Phycol. 46 (1), 74–87.
Tillmann, U., Salas, R., Gottschling, M., Krock, B., O'Driscoll, D., Elbrächter, M., 2012. *Amphidoma languida* sp. nov. (Dinophyceae) reveals a close relationship between *Amphidoma* and *Azadinium*. Protist 163 (5), 701–719.
Tillmann, U., Borel, C.M., Barrera, F., Lara, R., Krock, B., Almandoz, G.O., Witt, M., Trefault, N., 2016. *Azadinium poporum* from the Argentine Continental Shelf, Southwestern Atlantic, produces azaspiracid-2 and azaspiracid-2 phosphate. Harmful Algae 51, 40–55.
Tillmann, U., Jaén, D., Fernández, L., Gottschling, M., Witt, M., Blanco, J., Krock, B., 2017a. *Amphidoma languida* (Amphidomatacea, Dinophyceae) with a novel azaspiracid toxin profile identified as the cause of molluscan contamination at the Atlantic coast of southern Spain. Harmful Algae 62, 113–126.
Tillmann, U., Trefault, N., Krock, B., Parada-Pozo, G., De la Iglesia, R., Vásquez, M., 2017b. Identification of *Azadinium poporum* (Dinophyceae) in the Southeast Pacific: morphology, molecular phylogeny, and azaspiracid profile characterization. J. Plankton Res. 39 (2), 350–367.
Toebe, K., Joshi, A.R., Messtorff, P., Tillmann, U., Cembella, A., John, U., 2013. Molecular discrimination of taxa within the dinoflagellate genus *Azadinium*, the source of azaspiracid toxins. J. Plankton Res. 35 (1), 225–230.